Coherent elastic neutrino-nucleus scattering: electroweak and new physics probes

Dimitrios K. Papoulias

University of Athens, Greece

MPIK, Particle and Astroparticle Theory Seminar, June 20 2022

National and Kapodistrian
UNIVERSITY OF ATHENS

Ευρωπαϊκή Ένωση
European Social Fund

Operational Programme
Human Resources Development,
Education and Lifelong Learning

Co-financed by Greece and the European Union

ΕΣΠΑ
2014-2020
ανάπτυξη - εργασία - αλληλεγγύη

Outline

1. Introduction
   - Motivations
2. CEvNS searches within and beyond the Standard Model
   - Nuclear form factors and weak mixing angle
   - Non-standard interactions (NSIs)
   - Electromagnetic neutrino properties
3. Direct dark matter detection
   - WIMP-nucleus event rates
   - Neutrino backgrounds (neutrino floor)
4. Summary

What is CEνNS ?

CEνNS: Coherent elastic neutrino nucleus scattering

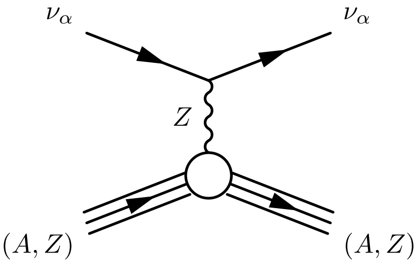

coherent: nucleon wavefunctions are in phase
elastic: target remains in the same energy state, $|g.s.\rangle \to |g.s.\rangle$ transitions

coherency limit: $|\vec{q}| \leq 1/R_{\textbf{nucleus}}$

- 3-momentum transfer $|\vec{q}| = \sqrt{2MT} = \sqrt{2E_\nu^2(1 - \cos\theta)}$
- M: nuclear mass
- E_ν: incident neutrino energy
- T: nuclear recoil energy
- θ: scattering angle

“An act of hubris”

First theorized in 1974 by D. Freedman

- 40 years until first detection August 2017
- Challenges of detection noted
- Other physics uses for CEvNS
    - Ex: Astrophysics

PHYSICAL REVIEW D VOLUME 9, NUMBER 5 1 MARCH 1974

Coherent effects of a weak neutral current

Daniel Z. Freedman†
National Accelerator Laboratory, Batavia, Illinois 60510
and Institute for Theoretical Physics, State University of New York, Stony Brook, New York 11790
(Received 15 October 1973; revised manuscript received 19 November 1973)

Our suggestion may be an act of hubris, because the inevitable constraints of interaction rate, resolution, and background pose grave experimental difficulties for elastic neutrino-nucleus scattering.

Experimentally the most conspicuous and most difficult feature of our process is that the only detectable reaction product is a recoil nucleus of low momentum. Ideally the apparatus should have sufficient resolution to identify and determine the momentum of the recoil nucleus and sufficient mass to achieve a reasonable interaction rate. Neutron background is a serious problem because elastic $n+A$ cross sections are generally large. Kinematics gives the relation

There is negligible neutrino-energy loss in nuclear scattering, but the transport cross section is large since the mean scattering angle is 70°. Most of the electron-scattering cross section (16) comes from large-relative-energy configurations, where there is small neutrino energy loss. Of course, inverse β decay is purely absorptive and instantaneously redeposits neutrino energy in the stellar medium.

Therefore we have a transport cross section due to nuclear scattering which is larger than the conventional transport and absorptive cross sections by a factor of 500 or more. At column densities where conventional mechanisms favor neutrino escape, the increased path length in the star due to multiple nuclear scattering makes absorption more probable, and stellar matter may become opaque to neutrinos at lower than conventional density.

Nuclear scattering may also be relevant to blow-off of the supernova mantle and to neutrino processes in the outer layers of a neutron star which consist of neutron-rich nuclei.[13] Since coherent neutrino-nucleus scattering is a straightforward consequence of a weak neutral current (assuming only $a_0 \neq 0$), a thorough study of these astrophysical speculations is worthwhile.

We are happy to acknowledge helpful conversations with several colleagues: V. Ashford, J. Bahcall, J. Bronzan, P. Franzini, R. Huson, J. Katz, B. Lee, J. Trefil, and J. Walker.

5

CEνNS has a really large cross section, but...

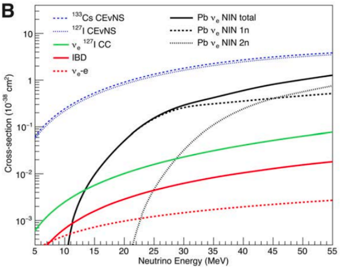

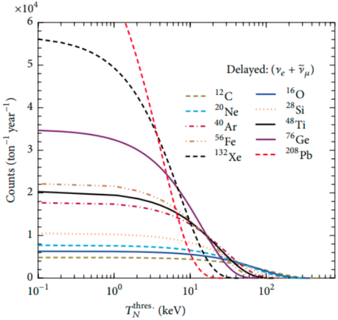

characteristic N^2 dependence

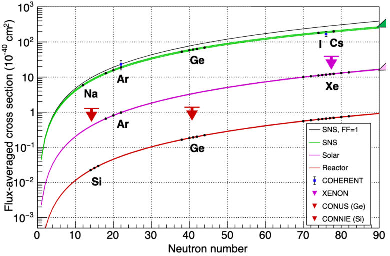

push-pull:

heavy nucleus $\rightarrow \sigma_{\text{CEvNS}} \rightarrow T_{\text{max}}$

$$T_{\text{max}} = \frac{2E_\nu^2}{M} \sim \text{keV}$$

CEνNS experiments worldwide

from M. Green: Aspen 2019 Winter Conference, March 2019

+ SBC (Mexico), vIOLETA (Argentina), ESS (Sweden), CCM (USA)

Observation of CEνNS by COHERENT

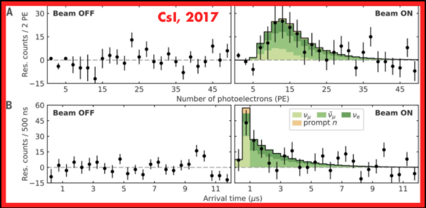

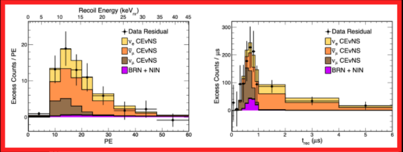

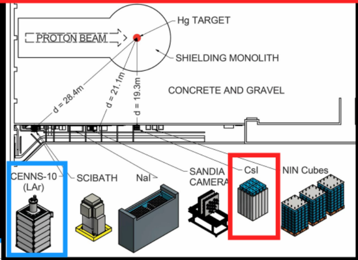

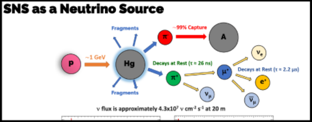

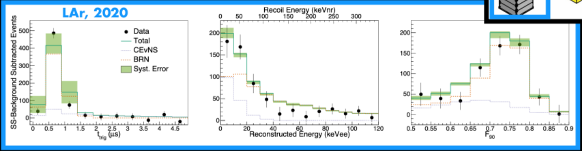

D. Akimov et al. (COHERENT). Science 357, 1123–1126 (2017)
D. Akimov et al. (COHERENT). 2110.07730
D. Akimov et al. (COHERENT). Phys. Rev. Lett. 126, 012002 (2021)
Daughhetee, BNL Physics Seminar 2020

CEνNS evidence using reactor antineutrinos

arXiv:2202.09672 [hep-ex]

Suggestive evidence for coherent elastic neutrino-nucleus scattering from reactor antineutrinos

J. Colaresi[1], J.I. Collar[2,*] T.W. Hossbach[3], C.M. Lewis[2], and K.M. Yocum[1]
[1]*Mirion Technologies Canberra, 800 Research Parkway, Meriden, CT, 06450, USA*
[2]*Enrico Fermi Institute, University of Chicago, Chicago, Illinois 60637, USA and*
[3]*Pacific Northwest National Laboratory, Richland, Washington 99354, USA*
(Dated: February 22, 2022)

The 96.4 day exposure of a 3 kg ultra-low noise germanium detector to the high flux of antineutrinos from a power nuclear reactor is described. A very strong preference for the presence of a coherent elastic neutrino-nucleus scattering (CEνNS) component in the data is found, when compared to a background-only model. No such effect is visible in 25 days of operation during reactor outages. The best-fit CEνNS signal is in good agreement with expectations based on a recent characterization of germanium response to sub-keV nuclear recoils. Deviations of order 60% from the Standard Model CEνNS prediction can be excluded using present data. Standing uncertainties in models of germanium quenching factor, neutrino energy spectrum, and background are examined.

ON/OFF data

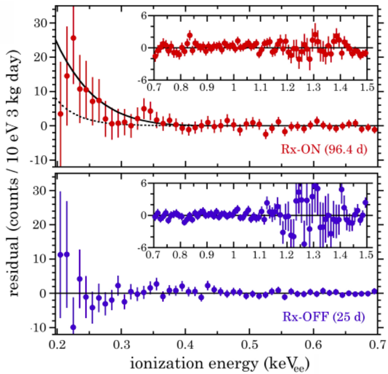

Neutrino sources: artificial sources (π^+ decay-at-rest)

Bunches of ~1 GeV protons on the Hg target with 60 Hz frequency

Proton bunch time profile with FWHM of ~350 ns

Total neutrino flux of $4.3 \cdot 10^7$ $cm^{-2}*s^{-1}$ at 20m

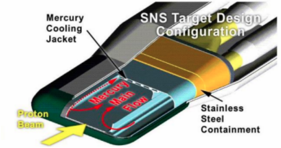

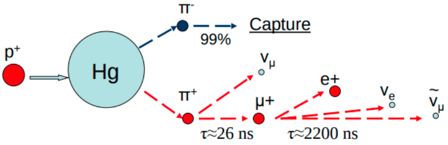

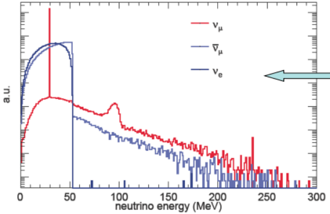

ν energy and timing suit well for CEvNS search

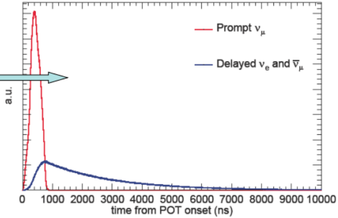

Neutrino sources: artificial sources (reactor neutrinos)

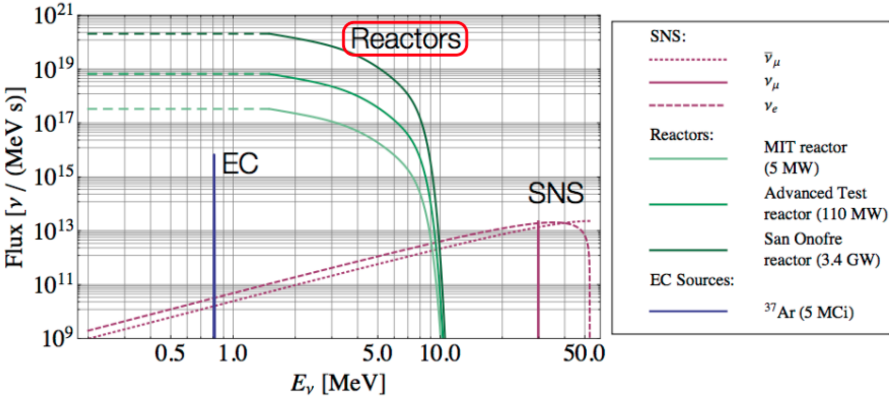

Nuclear reactor are very interesting neutrino source:

- High flux: $1\ \mathrm{GW_{th}} \rightarrow 2 \times 10^{20}\ \nu/s$
- Neutrino energy $< 10\,\mathrm{MeV}$: almost fully coherent

Neutrino backgrounds at direct dark matter detection experiments

Irreducible background

- **Solar neutrinos**
  [W. C. Haxton, R. G. Hamish Robertson, and A. M. Serenelli, Ann. Rev. Astron. Astrophys. **51** (2013), 21]
- **Atmospheric neutrinos**
  (FLUKA simulations)
  [G. Battistoni, A. Ferrari, T. Montaruli, and P. R. Sala, Astropart. Phys. **23** (2005) 526]
- **Diffuse Supernova Neutrinos (DSN)**
  [Horiuchi, Beacom, Dwek, PR **D79** (2009) 083013]

Type	$E_{\nu_{\max}}$ [MeV]	Flux $[\mathrm{cm}^{-2}\mathrm{s}^{-1}]$
pp	0.423	$(5.98 \pm 0.006) \times 10^{10}$
pep	1.440	$(1.44 \pm 0.012) \times 10^{8}$
hep	18.784	$(8.04 \pm 1.30) \times 10^{3}$
$^{7}\mathrm{Be}_{\mathrm{low}}$	0.3843	$(4.84 \pm 0.48) \times 10^{8}$
$^{7}\mathrm{Be}_{\mathrm{high}}$	0.8613	$(4.35 \pm 0.35) \times 10^{9}$
$^{8}\mathrm{B}$	16.360	$(5.58 \pm 0.14) \times 10^{6}$
$^{13}\mathrm{N}$	1.199	$(2.97 \pm 0.14) \times 10^{8}$
$^{15}\mathrm{O}$	1.732	$(2.23 \pm 0.15) \times 10^{8}$
$^{17}\mathrm{F}$	1.740	$(5.52 \pm 0.17) \times 10^{6}$

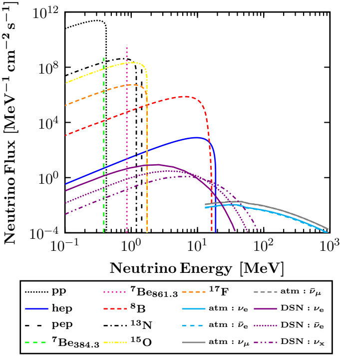

This talk will be about... but not restricted to...

SM and BSM CEνNS Neutrino Interactions

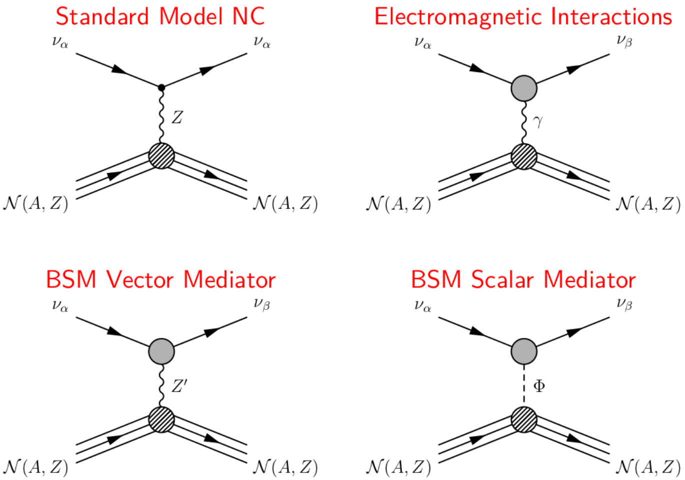

Standard Model physics

Standard Model CEνNS cross section

$$\left(\frac{d\sigma}{dT_A}\right)_{\mathrm{SM}} = \frac{G_F^2 m_A}{\pi}\left[\mathcal{Q}_V{}^2\left(1-\frac{m_A T_A}{2E_\nu^2}\right) + \cancelto{0}{\mathcal{Q}_A^2\left(1+\frac{m_A T_A}{2E_\nu^2}\right)}\right] F^2(Q^2)$$

[DKP, Kosmas: PRD 97 (2018)]

- **Nuclear form factor**

$$F(q^2) = \int e^{-i\vec{q}\cdot\vec{r}}\rho(r)\, d^3 r$$

where $\rho(r)$ is the charge density distribution

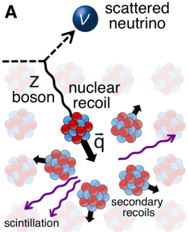

- weak mixing angle: $\sin^2\theta_W$ not measured with high precision at low energies

$$\mathcal{Q}_V = (1/2 - 2\sin^2\theta_W)Z - 1/2N \propto N^2$$

Nuclear rms radius

The CEnNS process as unique probe of the neutron density distribution of nuclei

The CEnNS process itself can be used to provide the first **model independent measurement of the neutron distribution radius**, which is basically unknown for most of the nuclei.

Even if it sounds strange, spatial distribution of neutrons inside nuclei is basically unknown!

The rms neutron distribution radius Rn and the difference between Rn and the rms radius Rp of the proton distribution (the so-called "**neutron skin**")

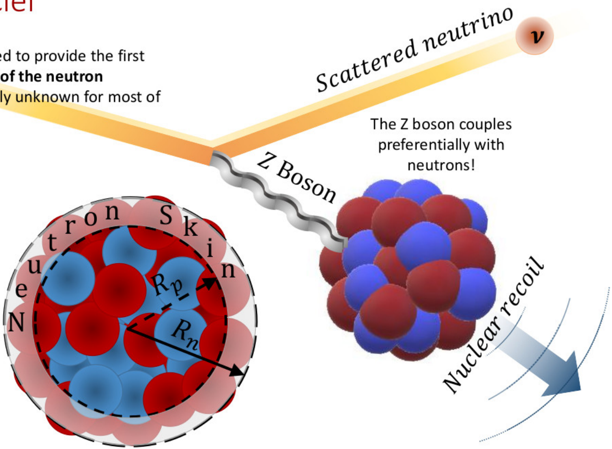

8

slide from: M. Cadeddu @ NuFact 2018

Phenomenological form factors (Klein-Nystrand)

Follows from the convolution of a Yukawa potential with range $a_k = 0.7$ fm over a Woods-Saxon distribution, approximated as a hard sphere with radius R_A.

$$F_{\mathrm{KN}} = 3\frac{j_1(QR_A)}{qR_A}\left[1+(Qa_k)^2\right]^{-1}$$

The rms radius is: $\langle R^2\rangle_{\mathrm{KN}} = 3/5R_A^2 + 6a_k^2$

[Klein, Nystrand, PRC 60 (1999) 014903]

[Miranda et al. JHEP 05 (2020) 130]

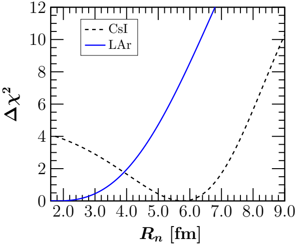

[Cadeddu et al., arXiv:2102.06153]

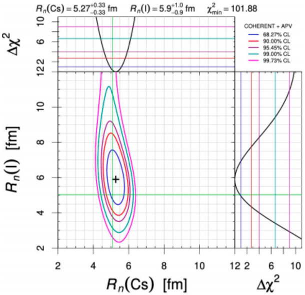

- **CEvNS data provides:** a data driven determination of the neutron rms radius
- **COHERENT (CsI) + APV (Cs):** can disentangle the Cs and I contributions

Impact of form factor on CEνNS: COHERENT exp.

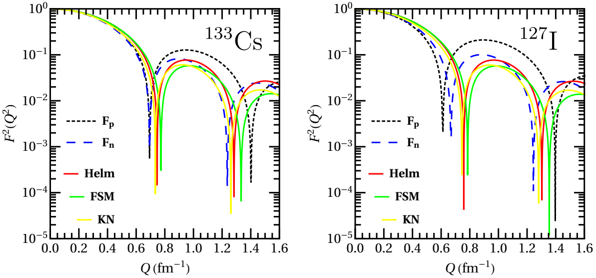

[DKP, Kosmas, Sahu, Kota, Hota PLB 800 (2020) 135133]

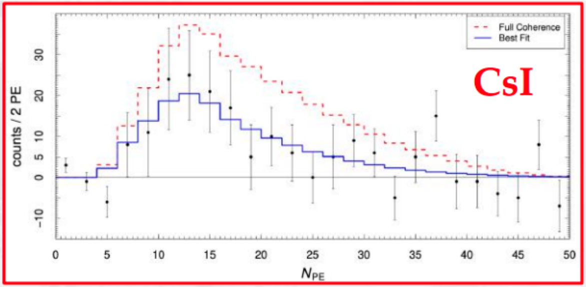

M. Cadeddu et al. - Phys.Rev.D 101 (2020) 3, 033004

Impact of form factor on CEνNS: COHERENT exp.

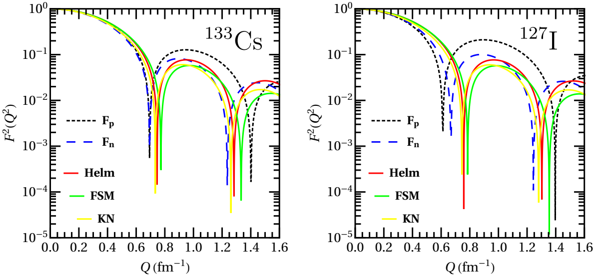

[DKP, Kosmas, Sahu, Kota, Hota PLB 800 (2020) 135133]

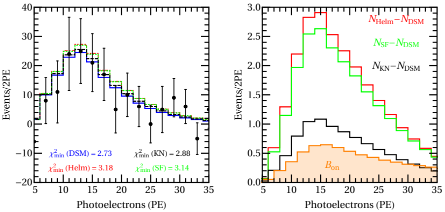

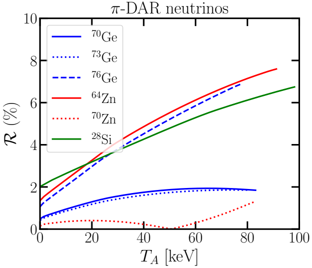

Up to 8% difference in the theoretical event rates

Standard Model precision tests (away from the Z-pole)

current situation from COHERENT

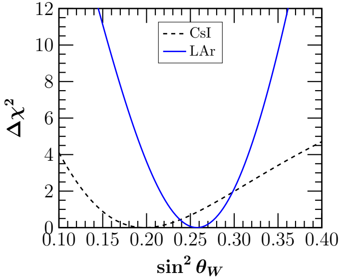

Miranda et al. JHEP 05 (2020) 130

including Dresden-II results

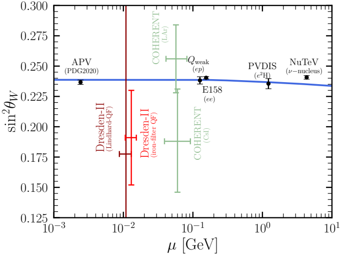

Aristizabal, De Romeri, DKP: arXiv: 2203.02414

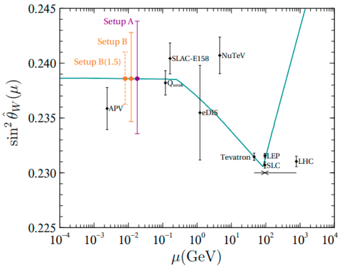

[SBC Collaboration] PRD 103 (2021)

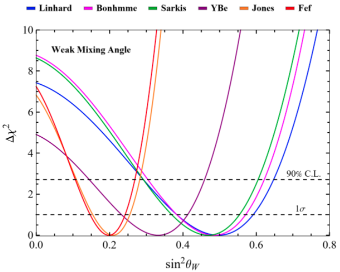

Khan, arXiv: 2203.08892

Incoherent vs. Coherent rates: πDAR and reactors

reactor neutrinos **πDAR neutrinos**

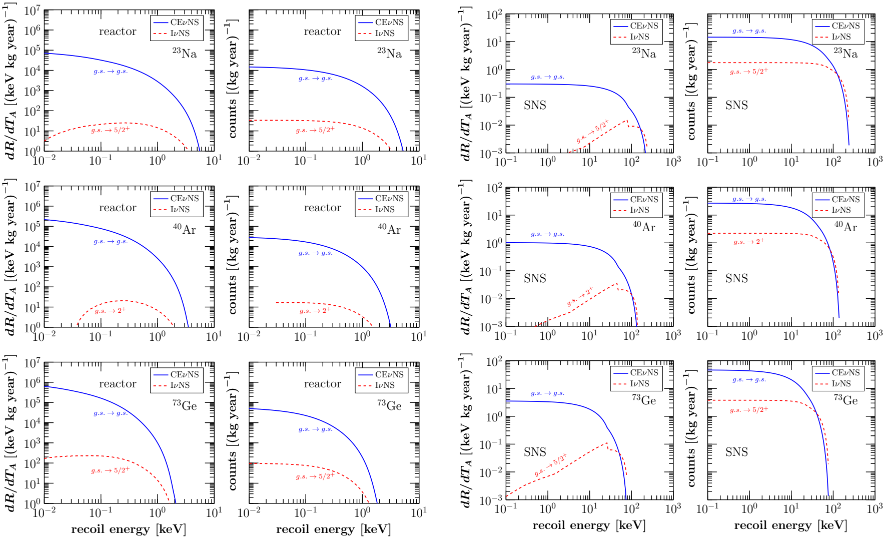

[Sahu, DKP, Kota, Kosmas, PRC 102 (2020) 3, 035501]

Incoherent vs. Coherent rates: solar neutrinos

Solar neutrinos

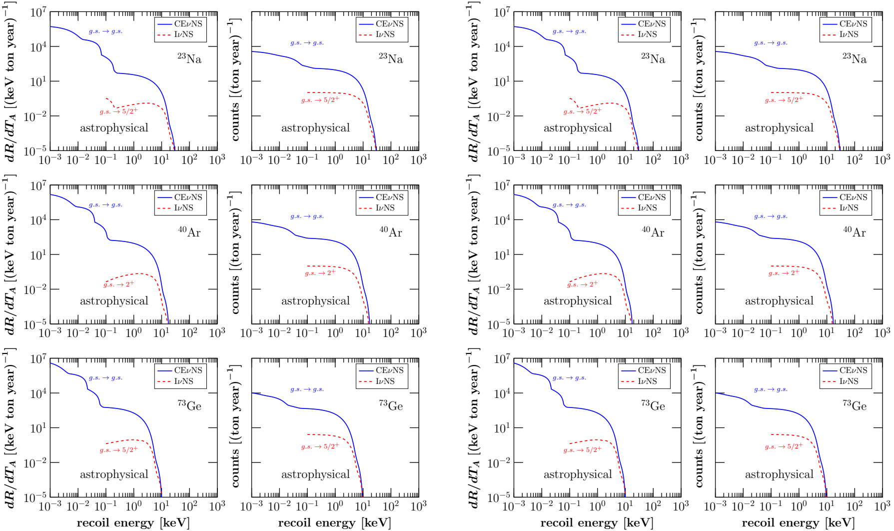

[Sahu, DKP, Kota, Kosmas, PRC 102 (2020) 3, 035501]

Non Standard Interactions (NSIs)

NSI Phenomenological description

Lagrangian describing non-standard neutrino interactions (NSI)

$$\mathcal{L}_{\mathrm{NSI}} = -2\sqrt{2}G_F \sum_{\substack{f=u,d \\ \alpha,\beta=e,\mu,\tau}} \epsilon_{\alpha\beta}^{fP} \left[\bar{\nu}_\alpha \gamma_\rho L \nu_\beta\right] \left[\bar{f}\gamma^\rho P f\right]$$

J. Barranco, O.G. Miranda, C.A. Moura and J.W.F. Valle, PRD 73 (2006) 113001

O.G. Miranda, M.A. Tortola and J.W.F. Valle, JHEP 0610 (2006) 008

- *flavour preserving non-universal (NU) terms* proportional to $\epsilon_{\alpha\alpha}^{fP}$.
- *flavour-changing (FC) terms* proportional to $\epsilon_{\alpha\beta}^{fP}$, $\alpha \neq \beta$.

The couplings with respect to the Fermi coupling constant G_F

are of vector and axial vector type, as

- vector couplings: $\epsilon_{\alpha\beta}^{fV} = \epsilon_{\alpha\beta}^{fL} + \epsilon_{\alpha\beta}^{fR}$
- axial-vector couplings: $\epsilon_{\alpha\beta}^{fA} = \epsilon_{\alpha\beta}^{fL} - \epsilon_{\alpha\beta}^{fR}$

S. Davidson et. al., JHEP 03 (2003) 011
J. Barranco, O.G. Miranda and T.I. Rashba, JHEP 0512 (2005) 021

K. Scholberg, PRD 73 (2006) 033005

NSI Analysis of COHERENT-CsI data

see also Giunti PRD 101, 035039 (2020)

- **vector NSI:** $\mathcal{O}_{\alpha\beta}^{qV} = (\bar{\nu}_\alpha \gamma^\mu L \nu_\beta)\,(\bar{q}\gamma_\mu P q)$
  CEνNS cross section becomes flavor dependent through the substitution $\mathcal{Q}_W^V \to \mathcal{Q}_{\rm NSI}^V$
- **NSI vector couplings**

$$\mathcal{Q}_{\rm NSI}^V = (2\epsilon_{\alpha\alpha}^{uV} + \epsilon_{\alpha\alpha}^{dV} + g_p^V) Z + (\epsilon_{\alpha\alpha}^{uV} + 2\epsilon_{\alpha\alpha}^{dV} + g_n^V) N + \sum_{\alpha,\beta} \left[(2\epsilon_{\alpha\beta}^{uV} + \epsilon_{\alpha\beta}^{dV}) Z + (\epsilon_{\alpha\beta}^{uV} + 2\epsilon_{\alpha\beta}^{dV}) N \right] .$$

- **Neutrino Generalized Interactions (NGI)**

$$\mathcal{L}_S \sim (\bar{\nu}\nu)\left[\bar{q}\left(C_S^q + i\gamma_5 D_S^q\right) q\right]$$
$$\mathcal{L}_P \sim (\bar{\nu}\gamma_5\nu)\left[\bar{q}\left(\gamma_5 C_P^q + i D_P^q\right) q\right]$$
$$\mathcal{L}_V \sim (\bar{\nu}\gamma^\mu\nu)\left[\bar{q}\left(\gamma_\mu C_V^q + i\gamma_\mu\gamma_5 D_V^q\right) q\right]$$
$$\mathcal{L}_A \sim (\bar{\nu}\gamma^\mu\gamma_5\nu)\left[\bar{q}\left(\gamma_\mu\gamma_5 C_A^q + i\gamma_\mu D_A^q\right) q\right]$$
$$\mathcal{L}_T \sim (\bar{\nu}\sigma^{\mu\nu}\nu)\left[\bar{q}\left(\sigma_{\mu\nu} C_T^q + i\sigma_{\mu\nu}\gamma_5 D_T^q\right) q\right]$$

Aristizabal, De Romeri, Rojas, PRD98 (2018) 075018

COHERENT Colab., arXiv:2110.07730

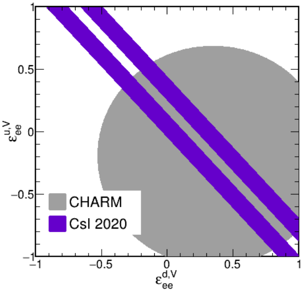

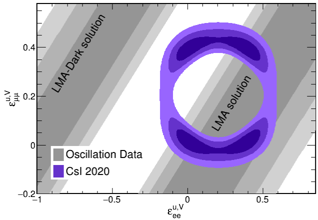

COHERENT-CsI vs. COHERENT-LAr data

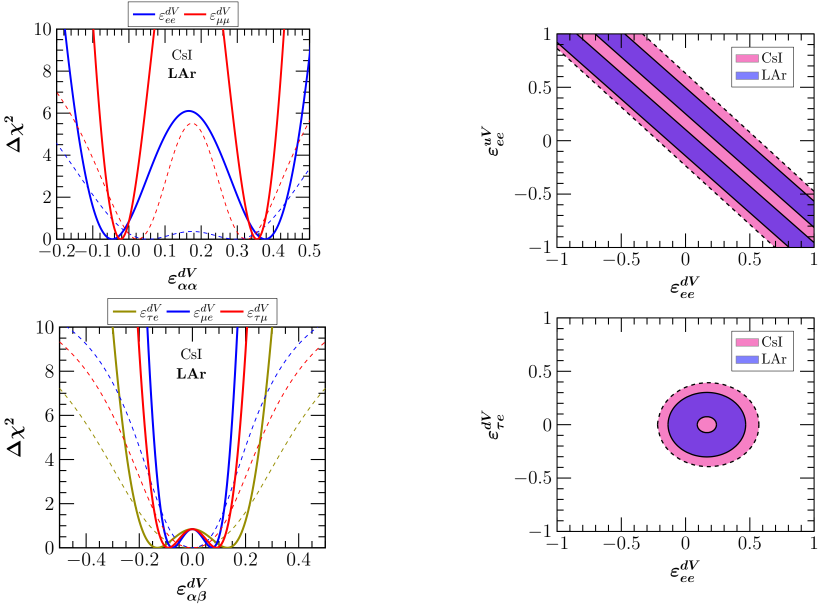

Miranda et al. JHEP 05 (2020) 130

$$\mathcal{L}_{\rm vec} = Z'_\mu \left(g_{Z'}^{qV} \bar{q}\gamma^\mu q + g_{Z'}^{\nu V} \bar{\nu}_L \gamma^\mu \nu_L \right) + \frac{1}{2} M_{Z'}^2 Z'_\mu Z'^\mu$$

- Z' **contribution to CEνNS cross section** Aristizabal, De Romeri, DKP: arXiv: 2203.02414

$$\left(\frac{d\sigma}{dT_N}\right)_{\rm SM+Z'} = \mathcal{G}_{Z'}^2(T_N) \frac{d\sigma_{\rm SM}}{dT_N} \,, \quad \text{with} \quad \mathcal{G}_{Z'} = 1 + \frac{1}{\sqrt{2} G_F} \frac{\mathcal{Q}_{Z'}}{\mathcal{Q}_W^V} \frac{g_{Z'}^{\nu V}}{2MT_N + M_{Z'}^2} \,,$$

- Z' **charge:** $\mathcal{Q}_{Z'} = \left(2g_{Z'}^{uV} + g_{Z'}^{dV}\right) Z + \left(g_{Z'}^{uV} + 2g_{Z'}^{dV}\right) N$

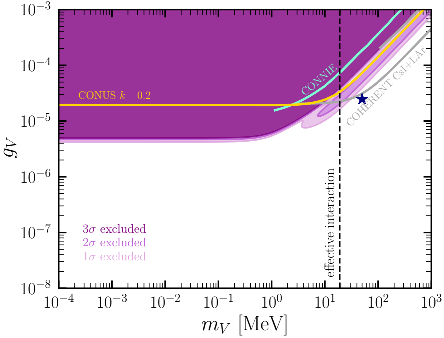

Light scalar mediator

$$\mathcal{L}_{\rm sc} = \phi\left(g_\phi^{qS}\bar{q}q + g_\phi^{\nu S}\bar{\nu}_R\nu_L + \text{H.c.}\right) - \frac{1}{2}M_\phi^2\phi^2$$

- ϕ **contribution to CEνNS cross section** Aristizabal, De Romeri, DKP: arXiv: 2203.02414

$$\left(\frac{d\sigma}{dT_N}\right)_{\rm scalar} = \frac{G_F^2 M^2}{4\pi}\frac{\mathcal{G}_\phi^2 M_\phi^4 T_N}{E_\nu^2\left(2MT_N + M_\phi^2\right)^2}F^2(T_N), \quad \text{with} \quad \mathcal{G}_\phi = \frac{g_\phi^{\nu S}\mathcal{Q}_\phi}{G_F M_\phi^2},$$

- **scalar charge:** $\mathcal{Q}_\phi = \sum_{\mathcal{N},q} g_\phi^{qS}\frac{m_\mathcal{N}}{m_q}f_{T,q}^{(\mathcal{N})}$

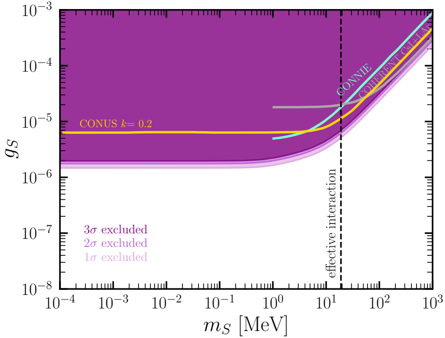

Neutrino Generalized Interactions (NGIs)

The Lagrangian describing NGIs, reads:

$$\mathscr{L}_{NGI} = \frac{G_F}{\sqrt{2}} \sum_{\substack{X=S,P,V,A,T \\ f=u,d \\ \alpha=e,\mu,\tau}} C_{\alpha,\alpha}^{f,P} \left[\bar{\nu}_\alpha \Gamma^X L \nu_\alpha\right] \left[\bar{f} \Gamma_X P f\right] \qquad \Gamma_X = \{\mathbb{I}, i\gamma_5, \gamma_\mu, \gamma_\mu\gamma_5, \sigma_{\mu\nu}\}$$

Dimensionless coefficients $C_{\alpha,\alpha}^{f,P}$ measure the relative strength of the new physics interaction X and are the order of $(\sqrt{2}/G_F)(g_X^2/(q^2+m_X^2))$.

Mediator	$\mathscr{L}_X$	Cross Section
Scalar	$\left[(g_{\nu S}\bar{\nu}_R\nu_L + h.c.) + \sum_{q=\{u,d\}} g_{qS}\bar{q}q\right] S + \frac{1}{2}m_S^2 S^2$	$\frac{m_N^2 E_{nr} Q_S^2}{4\pi E_\nu^2 \left(q^2+m_S^2\right)^2}$
Pseudoscalar	$\left[(g_{\nu P}\bar{\nu}_R\gamma_5\nu_L + h.c.) - i\sum_{q=\{u,d\}} g_{qP}\bar{q}\gamma_5 q\right] P + \frac{1}{2}m_P^2 P^2$	$\frac{m_N E_{nr}^2 Q_P^2}{8\pi E_\nu^2 \left(q^2+m_P^2\right)^2}$
Vector	$\left[g_{\nu V}\bar{\nu}_L\gamma_\mu\nu_L + \sum_{q=\{u,d\}} g_{qV}\bar{q}\gamma_\mu q\right] V^\mu + \frac{1}{2}m_V^2 V^\mu V_\mu$	$\left(1+\frac{Q_V}{\sqrt{2}G_F Q_V^{SM}\left(q^2+m_V^2\right)}\right)^2 \left[\frac{d\sigma}{dE_{nr}}\right]_{SM}^{\nu N}$
Axial Vector	$\left[g_{\nu A}\bar{\nu}_L\gamma_\mu\gamma_5\nu_L - \sum_{q=\{u,d\}} g_{qA}\bar{q}\gamma_\mu\gamma_5 q\right] A^\mu + \frac{1}{2}m_A^2 A^\mu A_\mu$	$\frac{m_N Q_A^2 (2E_\nu^2+m_N E_{nr})}{4\pi E_\nu^2 \left(q^2+m_A^2\right)^2}$
Tensor	$\left[g_{\nu T}\bar{\nu}_R\sigma_{\rho\delta}\nu_L - \sum_{q=\{u,d\}} g_{qT}\bar{q}\sigma_{\rho\delta} q\right] T^{\rho\delta} + \frac{1}{2}m_T^2 T^{\rho\delta}T_{\rho\delta}$	$\frac{m_N Q_T^2 (4E_\nu^2-m_N E_{nr})}{2\pi E_\nu^2 \left(q^2+m_T^2\right)^2}$

TABLE I: Novel interactions $X = \{S, P, V, A, T\}$ and corresponding differential CEνNS cross sections considered in the present work. Due to interference, the V interaction is the only case that includes the SM contribution, while the S, P, A, T cases acquire contributions from new physics only, as shown in the cross sections (see the text for more details).

Projected NGI sensitivity

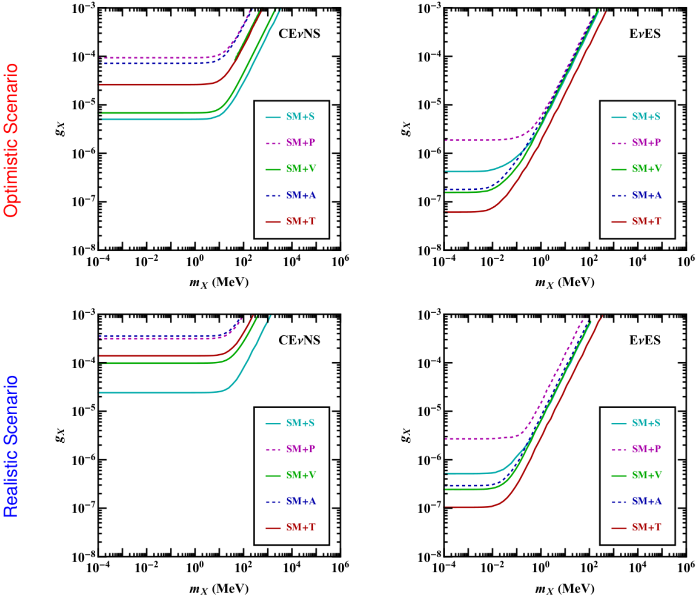

Majumdar, DKP, Srivastava: arXiv: 2112.03309 [hep-ph]

$B - L$ and $L_\mu - L_\tau$ sensitivity

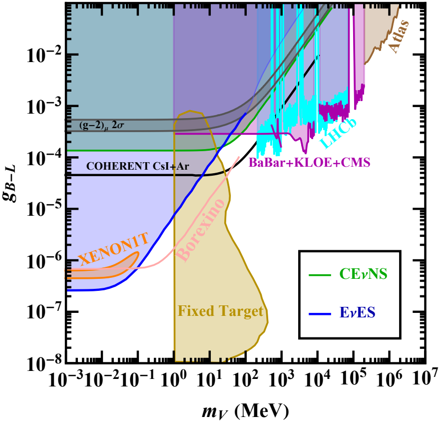

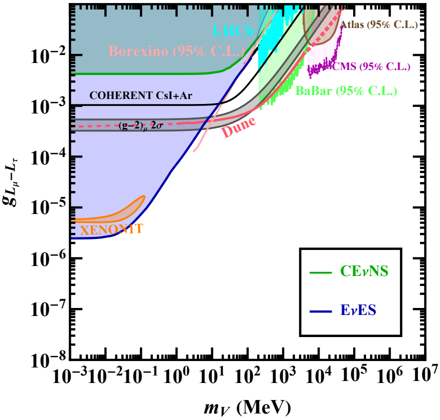

Majumdar, DKP, Srivastava: arXiv: 2112.03309 [hep-ph]

Electromagnetic neutrino properties

Electromagnetic interactions

For neutrinos the electric charge is zero and there are no electromagnetic interactions at tree level. However, such interactions can arise at the quantum level from loop diagrams at higher order of the perturbative expansion of the interaction.

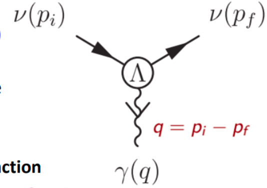

- **Effective Hamiltonian** $\mathcal{H}^{(\nu)}_{\text{em}}(x) = j^{(\nu)}_{\mu}(x)A^{\mu}(x) = \sum_{k,j=1} \overline{\nu_k}(x)\Lambda^{kj}_{\mu}\nu_j(x)A^{\mu}(x)$

- We are interested in the neutrino part of the amplitude which is given by the following matrix element $\langle \nu_f(p_f)|j^{(\nu)}_{\mu}(0)|\nu_i(p_i)\rangle = \overline{u_f}(p_f)\Lambda^{fi}_{\mu}(q)u_i(p_i)$

- The electromagnetic properties of neutrinos are embedded by the **vertex function**

$$\Lambda_{\mu}(q) = \left(\gamma_{\mu} - q_{\mu}\not{q}/q^2\right)\left[F_Q(q^2) + F_A(q^2)q^2\gamma_5\right] - i\sigma_{\mu\nu}q^{\nu}\left[F_M(q^2) + iF_E(q^2)\gamma_5\right]$$

Lorentz-invariant form factors: charge, anapole, magnetic, electric

$q^2 = 0 \Longrightarrow$ $\mathfrak{q}$, a, μ, ε

Charge and anapole moment — Magnetic and electric dipole moments

[C. Giunti, A. Studenikin, Neutrino electromagnetic interactions: A window to new physics, Rev Mod Phys, 87, 531 (2015), Arxiv:1403.6344*]*

taken from M. Cadeddu, Magnificent CEvNS 2020

Electromagnetic contribution to CEνNS cross section

The Electromagnetic CEνNS cross section reads [Vogel, Engel.: PRD 39 [1989] 3378]

$$\left(\frac{d\sigma}{dT_A}\right)_{\mathrm{EM}} = \frac{\pi a_{\mathrm{EM}}^2 \mu_\nu^2 Z^2}{m_e^2} \left(\frac{1}{T_A} - \frac{1}{E_\nu}\right) F_Z^2(Q^2)$$

- can be dominant for sub-keV threshold experiments
- may lead to detectable distortions of the recoil spectrum

The helicity preserving SM cross section adds incoherently with the helicity-violating EM cross section

$$\left(\frac{d\sigma}{dT_A}\right)_{\mathrm{tot}} = \left(\frac{d\sigma}{dT_A}\right)_{\mathrm{SM}} + \left(\frac{d\sigma}{dT_A}\right)_{\mathrm{EM}}$$

μ_ν^2 is an effective (process-dependent) neutrino magnetic moment relevant to a given neutrino beam (reactor, SNS, etc.)

Analysis of the COHERENT data: EM properties

- **Neutrino magnetic moment**

$$\left(\frac{d\sigma}{dT_A}\right)_{\rm tot} = \left(\frac{d\sigma}{dT_A}\right)_{\rm SM} + \left(\frac{d\sigma}{dT_A}\right)_{\rm EM}$$

$$\left(\frac{d\sigma}{dT_A}\right)_{\rm EM} = \frac{\pi a_{\rm EM}^2 \mu_\nu^2\, Z^2}{m_e^2}\left(\frac{1}{T_A} - \frac{1}{E_\nu}\right) F_Z^2(Q^2)$$

[Vogel, Engel: PRD 39 [1989] 3378]

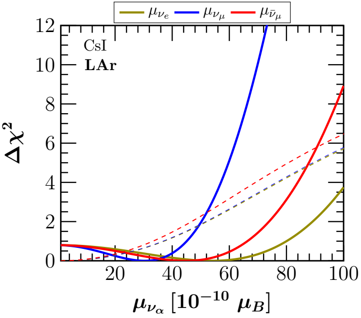

Miranda et al. JHEP 05 (2020) 130

- **Neutrino charge radius**

$$\sin^2\theta_W \to \sin^2\overline{\theta_W} + \frac{\sqrt{2}\pi a_{\rm EM}}{3G_F}\langle r_{\nu_\alpha}^2\rangle\,.$$

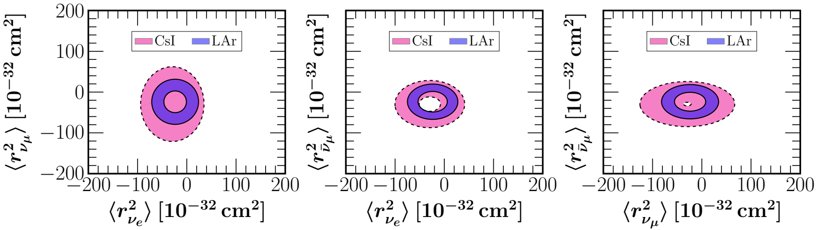

Electromagnetic contribution to CEνNS cross section

The Electromagnetic CEνNS cross section reads [Vogel, Engel.: PRD 39 [1989] 3378

$$\frac{\mathrm{d}\sigma_{\nu\mathcal{N}\to\nu\mathcal{N}}}{\mathrm{d}E_r} = \frac{\pi a_{\mathrm{EM}}^2 \mu_\nu^2 \, Z^2}{m_e^2}\left[\frac{1}{E_r} - \frac{1}{E_\nu}\right] F_p^2(Q^2)$$

Massive sterile neutrino in the final state?

[McKeen, Pospelov: PRD82 (2010)]

$$\frac{\mathrm{d}\sigma_{\nu\mathcal{N}\to\nu_s\mathcal{N}}}{\mathrm{d}E_r} = \frac{\pi a_{\mathrm{EM}}^2 \mu_\nu^2 \, Z^2}{m_e^2}\left[\frac{1}{E_r} - \frac{1}{E_\nu} - \frac{m_4^2}{2E_\nu E_r M}\left(1 - \frac{E_r}{2E_\nu} + \frac{M}{2E_\nu}\right) + \frac{m_4^4(E_r - M)}{8E_\nu^2 E_r^2 M^2}\right] F_p^2(Q^2)$$

The helicity preserving SM cross section adds incoherently with the helicity-violating EM cross section

$$\left(\frac{\mathrm{d}\sigma}{\mathrm{d}E_r}\right)_{\mathrm{tot}} = \left(\frac{\mathrm{d}\sigma}{\mathrm{d}E_r}\right)_{\mathrm{SM}} + \left(\frac{\mathrm{d}\sigma}{\mathrm{d}E_r}\right)_{\mathrm{EM}}$$

$\boldsymbol{\mu_\nu^2}$ is the effective neutrino magnetic moment in the mass basis relevant to a given neutrino beam (reactor, πDAR, solar etc.)

Active-sterile transitions via magnetic moment

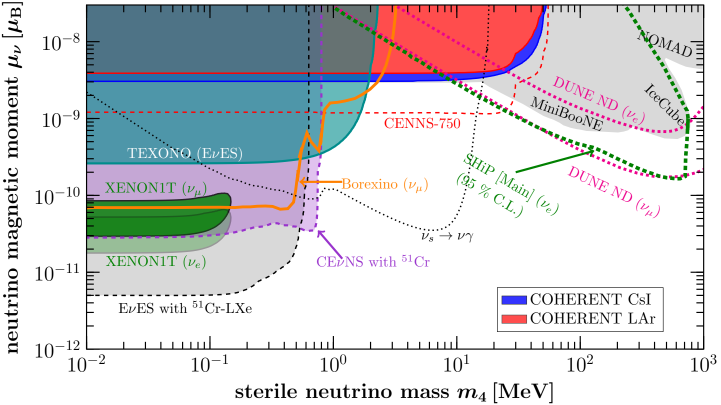

[Miranda, Papoulias, Sanders, Tórtola, Valle: 2109.09545 [hep-ph]]

- COHERENT can cover a large space in sterile mass, previously unexplored
- Reactor experiments are more sensitive to the magnetic moment
- ^{51}Cr-based neutrino experiments can probe XENON1T

- complementarity with large-scale experiments (DUNE, IceCube, NOMAD, SHiP)

see also P. Bolton et al. arXiv: 2110.02233 [hep-ph]

Electromagnetic neutrino vertex

Dirac neutrinos: $H_{\mathsf{EM}}^{\mathrm{D}} = \frac{1}{2}\bar{\nu}_R \lambda \sigma^{\alpha\beta} \nu_L F_{\alpha\beta} + \mathrm{h.c.}$

- $\lambda = \mu - i\epsilon$ is an arbitrary complex matrix
- $\mu = \mu^\dagger$ and $\epsilon = \epsilon^\dagger$.

Majorana neutrinos: $H_{\mathsf{EM}}^{\mathrm{M}} = -\frac{1}{4}\nu_L^{\mathsf{T}} C^{-1} \lambda \sigma^{\alpha\beta} \nu_L F_{\alpha\beta} + \mathrm{h.c.}$

- $\lambda = \mu - i\epsilon$: antisymmetric complex matrix $(\lambda_{\alpha\beta} = -\lambda_{\beta\alpha})$
- $\mu^{\mathsf{T}} = -\mu$ and $\epsilon^{\mathsf{T}} = -\epsilon$ are two imaginary matrices.
- three complex or six real parameters are required

In contrast to the Dirac case, vanishing diagonal moments are implied for Majorana neutrinos, $\mu_{ii}^{\mathrm{M}} = \epsilon_{ii}^{\mathrm{M}} = 0$.

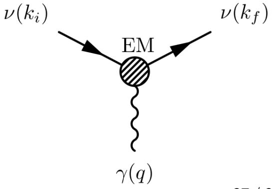

[Schechter, Valle: PRD 24 (1981), PRD 25 (1982)]

Effective neutrino magnetic moment @ experiments

$\boldsymbol{\mu_\nu^2}$ is expressed in terms of the neutrino magnetic moment matrix and the amplitudes of positive and negative helicity states 3−vectors $\mathfrak{a}_+$ and $\mathfrak{a}_-$,

- In the flavor basis one finds [Grimus, Schwetz: Nucl. Phys. B587 (2000)]

$$\left(\mu_\nu^F\right)^2 = \mathfrak{a}_-^\dagger \lambda^\dagger \lambda \mathfrak{a}_- + \mathfrak{a}_+^\dagger \lambda \lambda^\dagger \mathfrak{a}_+ \,,$$

Introducing the transformations (U is the lepton mixing matrix)

$$\tilde{\mathfrak{a}}_- = U^\dagger \mathfrak{a}_-, \qquad \tilde{\mathfrak{a}}_+ = U^\mathsf{T} \mathfrak{a}_+, \qquad \tilde{\lambda} = U^\mathsf{T} \lambda U \,,$$

- In the mass basis reads

$$\left(\mu_\nu^M\right)^2 = \tilde{\mathfrak{a}}_-^\dagger \tilde{\lambda}^\dagger \tilde{\lambda} \tilde{\mathfrak{a}}_- + \tilde{\mathfrak{a}}_+^\dagger \tilde{\lambda} \tilde{\lambda}^\dagger \tilde{\mathfrak{a}}_+$$

- Λ_i: entries of the transition magnetic moment matrix with $\lambda_{\alpha\beta} = \varepsilon_{\alpha\beta\gamma} \Lambda_\gamma$
- three complex or six real parameters (3 moduli + 3 phases)

TMMs in flavor & mass basis @ reactor facilities

Reactor antineutrinos: $\bar{\nu}_e$ (with $\mathfrak{a}^1_+ = 1$)

- flavor basis

$$\left(\mu^F_{\bar{\nu}_e,\,\mathrm{reactor}}\right)^2 = |\Lambda_\mu|^2 + |\Lambda_\tau|^2$$

where $|\Lambda_\mu|$ and $|\Lambda_\tau|$ are the elements of the neutrino TMM matrix λ describing the corresponding conversions from the electron antineutrino to the muon and tau neutrino states

- mass basis [Cañas et al.: PLB 753 (2016)]

$$\begin{aligned}\left(\mu^M_{\bar{\nu}_e,\,\mathrm{reactor}}\right)^2 =& |\boldsymbol{\Lambda}|^2 - c_{12}^2 c_{13}^2 |\Lambda_1|^2 - s_{12}^2 c_{13}^2 |\Lambda_2|^2 - s_{13}^2 |\Lambda_3|^2 \\ & - c_{13}^2 \sin 2\theta_{12} |\Lambda_1||\Lambda_2| \cos \xi_3 \\ & - c_{12} \sin 2\theta_{13} |\Lambda_1||\Lambda_3| \cos(\delta_{\mathrm{CP}} - \xi_2) \\ & - s_{12} \sin 2\theta_{13} |\Lambda_2||\Lambda_3| \cos(\delta_{\mathrm{CP}} - \xi_1)\,,\end{aligned}$$

with $|\boldsymbol{\Lambda}|^2 = |\Lambda_1|^2 + |\Lambda_2|^2 + |\Lambda_3|^2$ and

phase redefinition: $\xi_1 = \zeta_3 - \zeta_2$, $\xi_2 = \zeta_3 - \zeta_1$ and $\xi_3 = \zeta_1 - \zeta_2$

Interference between magnetic and weak interactions

Non-zero contribution for massive final state neutrinos

[Grimus, Stockinger: PRD 57 [1998]]

$$\left(\frac{\mathrm{d}\sigma_{\bar{\nu}_e e^- \to \nu_s e^-}}{\mathrm{d}E_r}\right)^{\text{interf}} = \frac{\alpha_{\text{em}} G_F\, m_4}{\sqrt{2}E_\nu\, m_e} \mathrm{Re}\left[\sum_{j,n} e^{-i\frac{\Delta m^2_{jn} L}{2E_\nu}} U_{ej} U^*_{en} \tilde{\lambda}_{j4} \left(\frac{m_e}{E_\nu} - \frac{E_r}{E_\nu}\right) Z^{V*}_{n4} + \left(2 - \frac{E_r}{E_\nu}\right) Z^{A*}_{n4}\right]$$

- $Z^{V,A}_{jk} = U_{ej} U^*_{ek} + \delta_{jk} \tilde{g}_{V,A}$ with $\tilde{g}_V = -1/2 + 2\sin^2\theta_W$ and $\tilde{g}_A = -1/2$
- For $\nu_e - e^-$ scattering: $\tilde{g}_A \to -\tilde{g}_A$ and $Z^{V,A}_{jk} \to (Z^{V,A}_{jk})^*$

- incident ν_e or $\bar{\nu}_e$: $\frac{\mathrm{d}\sigma}{\mathrm{d}E_r} \propto \frac{m_4}{m_e} \sin 2\theta_{14}$
- incident ν_μ or $\bar{\nu}_\mu$, $\frac{\mathrm{d}\sigma}{\mathrm{d}E_r} \propto \frac{m_4}{m_e} c_{14} s^2_{24}$
- interference is vanishing for the case of solar neutrinos

For CEνNS one needs the replacements

- $\tilde{\lambda}_{ij} \to \tilde{\lambda}_{ij} Z F_p(q^2)$
- $\tilde{g}_V \to \mathcal{Q}_V$ and $\tilde{g}_A \to \mathcal{Q}_A$
- $m_e \to M$

Current limits on NMM

limits @ 90% C.L.

Type	Experiment	Eff. coupling	90% CL limit (range)
Reactor	GEMMA [7]	μ_{ν_e}	2.9×10^{-11}
π-DAR	LSND [2]	μ_{ν_μ}	6.8×10^{-10}
π-DAR	DONUT [3]	μ_{ν_τ}	3.9×10^{-7}
Solar	Borexino [6]	μ_{ν_e}	2.8×10^{-11}
Solar	XENON1T [8]	μ_{ν_e}	$[1.4, 2.9] \times 10^{-11}$

Dirac vs. Majorana

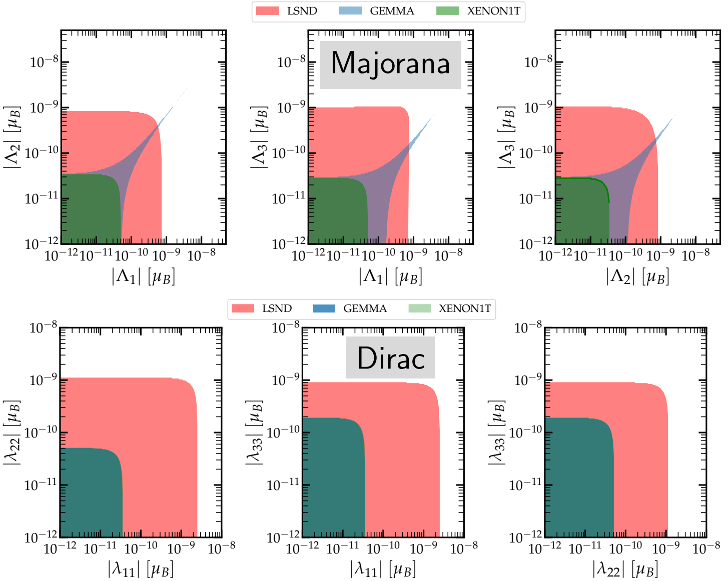

neutrino milli-charge

$$\sin^2\theta_W \to \sin^2\theta_W \left(1 - \frac{\pi a_{em}}{\sqrt{2}\sin^2\theta_W G_F M T} Q_{\alpha\alpha}\right)$$

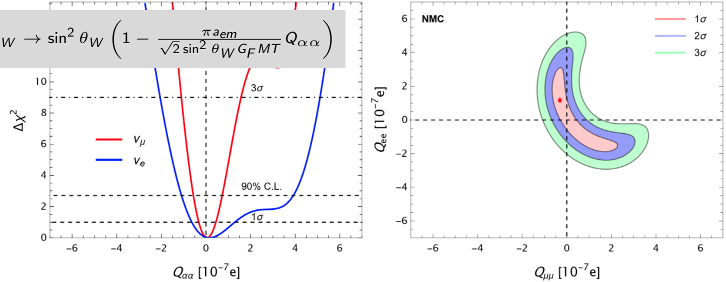

anapole moment

$$\sin^2\theta_W \to \sin^2\theta_W \left(1 - \frac{3\pi a_{em}}{\sqrt{2}\sin^2\theta_W G_F} a_{\nu\alpha}\right)$$

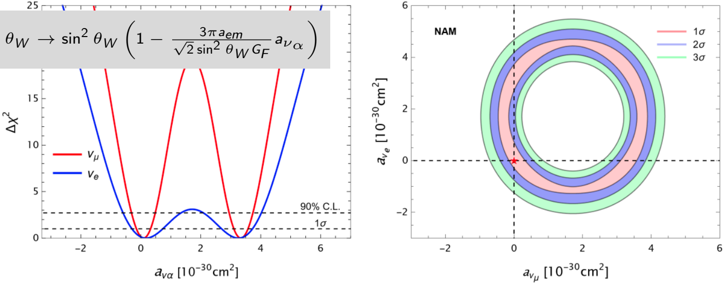

[A. Khan: 2201.10578 [hep-ph]]

Neutrino Backgrounds at Dark Matter Detectors

WIMP-nucleus scattering

weakly interacting massive particles (WIMPs)

Differential event rate as a function of E_r

$$\frac{dR_W}{dE_r} = \varepsilon \frac{\rho_0 \sigma_{\mathrm{SI}}(q)}{2 m_\chi \mu^2} \int_{|\boldsymbol{v}|>v_{\min}} d^3 v \, \frac{f(\boldsymbol{v})}{v}$$

[Lewin and Smith: Astropart. Phys. 6 (1996)]

- $\rho_0 = 0.3\ \mathrm{GeV}/\mathrm{cm}^2$ local Halo DM density
- $\sigma_{\mathrm{SI}}(q) = \frac{\mu^2}{\mu_n^2} \left[Z F_p(q) + (A-Z) F_n(q)\right]^2 \sigma_{\chi-n}$
  Spin-independent WIMP-nucleus scattering
- m_χ: WIMP mass
- $\mu = m_\chi m_N / (m_\chi + m_N)$: WIMP-nucleus reduced mass
- $f(v) = \begin{cases} \frac{1}{N_{\mathrm{esc}}} \left(\frac{3}{2\pi\sigma_v^2}\right)^{3/2} e^{-3\boldsymbol{v}^2/2\sigma_v^2} & \text{for} \quad v < v_{\mathrm{esc}} \\ 0 & \text{for} \quad v > v_{\mathrm{esc}} \end{cases}$ (Maxwell distribution)

Neutrino events at dark matter direct detection exps

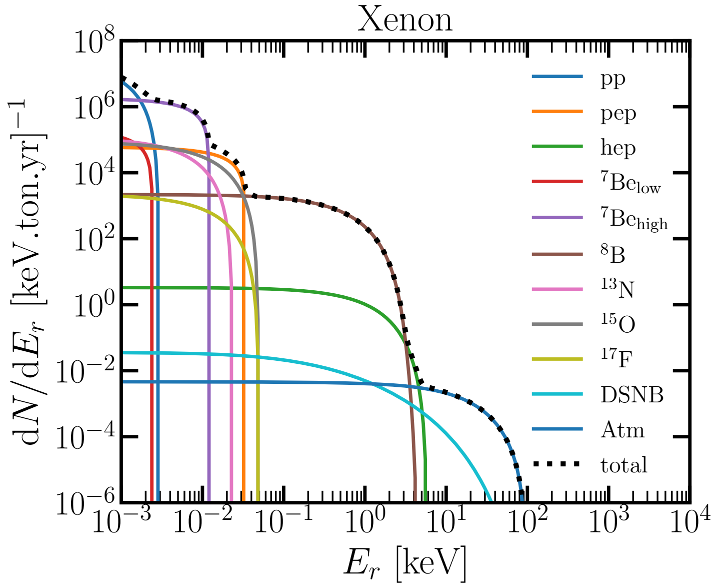

Neutrino vs. WIMP events

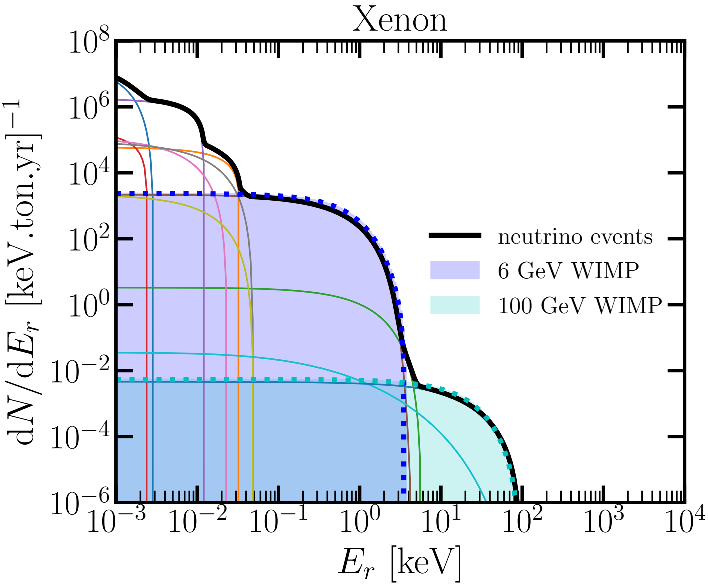

Conclusions: CEvNS complementarity to dark matter searches

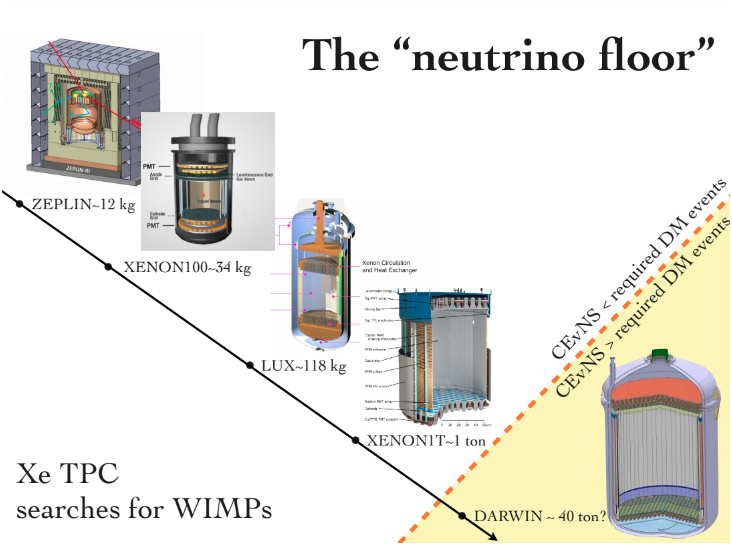

slide taken from: C. O'Hare Magnificent CEvNS 2020 Workshop

Statistical analysis

Likelihood

[Billard, Strigari, Figueroa-Feliciano PRD 89(2014)]

$$\mathcal{L}(m_\chi, \sigma_{\chi-n}, \Phi, \mathcal{P}) = \prod_{i=1}^{n_{\text{bins}}} P(N^i_{\text{Exp}}, N^i_{\text{Obs}}) \times \prod_{\alpha=1}^{n_\nu} G(\phi_\alpha, \mu_\alpha, \sigma_\alpha)$$

- Poisson distribution $P(k,\lambda) = \frac{\lambda^k e^{-\lambda}}{k!}$
- Gauss distribution $G(x,\mu,\sigma^2) = \frac{1}{\sigma\sqrt{2\pi}} e^{-\frac{1}{2}\left(\frac{x-\mu}{\sigma}\right)^2}$
- $N^i_{\text{Exp}} = N^i_\nu(\Phi_\alpha)$
- $N^i_{\text{Obs}} = \sum_\alpha N^i_\nu(\Phi_\alpha) + N^i_W$
- $\lambda(0) = \frac{\mathcal{L}_0}{\mathcal{L}_1}$ where $\mathcal{L}_0$ is the minimized function
- statistical significance: $\mathcal{Z} = \sqrt{-2 \ln \lambda(0)}$.
  e.g. $\mathcal{Z} = 3$ corresponds to 90% C.L.

Neutrino flux normalizations & uncertainties					
Type	Norm $[\mathrm{cm}^{-2}\cdot\mathrm{s}^{-1}]$	Unc.	Type	Norm $[\mathrm{cm}^{-2}\cdot\mathrm{s}^{-1}]$	Unc.
^{7}Be (0.38 MeV)	4.84×10^8	3%	^{7}Be (0.86 MeV)	4.35×10^9	3%
pep	1.44×10^8	1%	pp	5.98×10^{10}	0.6%
^{8}B	5.25×10^6	4%	hep	7.98×10^3	30%
^{13}N	2.78×10^8	15%	^{15}O	2.05×10^8	17%
^{17}F	5.29×10^6	20%	DSNB	86	50%
Atm	10.5	20%	—	—	—

Statistical analysis

Likelihood

[Billard, Strigari, Figueroa-Feliciano PRD 89(2014)]

$$\mathcal{L}(m_\chi, \sigma_{\chi-n}, \Phi, \mathcal{P}) = \prod_{i=1}^{n_{\text{bins}}} P(N^i_{\text{Exp}}, N^i_{\text{Obs}}) \times \prod_{\alpha=1}^{n_\nu} G(\phi_\alpha, \mu_\alpha, \sigma_\alpha)$$

- Poisson distribution $P(k,\lambda) = \frac{\lambda^k e^{-\lambda}}{k!}$
- Gauss distribution $G(x,\mu,\sigma^2) = \frac{1}{\sigma\sqrt{2\pi}} e^{-\frac{1}{2}\left(\frac{x-\mu}{\sigma}\right)^2}$
- $N^i_{\text{Exp}} = N^i_\nu(\Phi_\alpha)$
- $N^i_{\text{Obs}} = \sum_\alpha N^i_\nu(\Phi_\alpha) + N^i_W$
- $\lambda(0) = \frac{\mathcal{L}_0}{\mathcal{L}_1}$ where $\mathcal{L}_0$ is the minimized function
- statistical significance: $\mathcal{Z} = \sqrt{-2\ \ln \lambda(0)}$.
  e.g. $\mathcal{Z} = 3$ corresponds to 90% C.L.

Discovery limit: smallest WIMP cross section for which a given experiment has a 90% probability of detecting a WIMP signal at $\leq 3\sigma$.

Profile likelihood ratio: test against the null hypothesis H_0 (CEvNS background only) vs. the alternative hypothesis H_1 (WIMP signal + CEvNS background).

Statistical analysis

Likelihood

[Aristizabal, De Romeri, Flores, DKP: 2109.03247 [hep-ph]]

$$\mathcal{L}(m_\chi, \sigma_{\chi-n}, \Phi, \mathcal{P}) = \prod_{i=1}^{n_{\text{bins}}} P(N^i_{\text{Exp}}, N^i_{\text{Obs}}) \times \boxed{G(\mathcal{P}_i, \mu_{\mathcal{P}_i}, \sigma_{\mathcal{P}_i})} \times \prod_{\alpha=1}^{n_\nu} G(\phi_\alpha, \mu_\alpha, \sigma_\alpha)$$

- Poisson distribution $P(k, \lambda) = \frac{\lambda^k e^{-\lambda}}{k!}$
- Gauss distribution $G(x, \mu, \sigma^2) = \frac{1}{\sigma\sqrt{2\pi}} e^{-\frac{1}{2}\left(\frac{x-\mu}{\sigma}\right)^2}$
- $N^i_{\text{Exp}} = N^i_\nu(\Phi_\alpha, \mathcal{P}_i)$
- $N^i_{\text{Obs}} = \sum_\alpha N^i_\nu(\Phi_\alpha, \mathcal{P}_i) + N^i_W(\mathcal{P}_i)$
- $\lambda(0) = \frac{\mathcal{L}_0}{\mathcal{L}_1}$ where $\mathcal{L}_0$ is the minimized function
- statistical significance: $\mathcal{Z} = \sqrt{-2 \ln \lambda(0)}$.
  e.g. $\mathcal{Z} = 3$ corresponds to 90% C.L.

Parameter ($\mathcal{P}$)	Normalization (μ)	Uncertainty
R_n	4.78 fm	10%
$\sin^2\theta_W$	0.2387	10%

Neutrino floor: SM uncertainties (weak mixing angle)

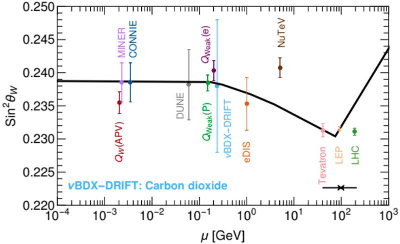

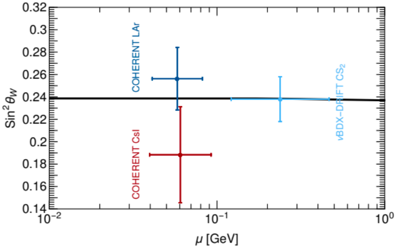

[Aristizabal et al. PRD 104 (2021)]

- $\mathcal{Q}_W = (\frac{1}{2} - 2\sin^2\theta_W)Z - \frac{1}{2}N$
- assume 10% uncertainty
- vary around the central value: $\sin^2\theta_W = 0.2387$

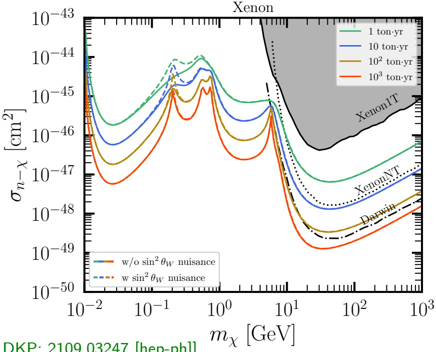

[Aristizabal, De Romeri, Flores, DKP: 2109.03247 [hep-ph]]

Neutrino floor: SM uncertainties (nuclear physics)

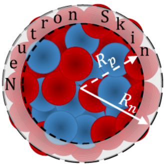

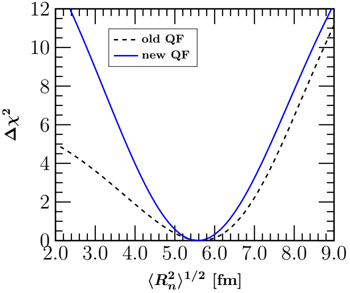

[DKP: PRD 102 (2020)]

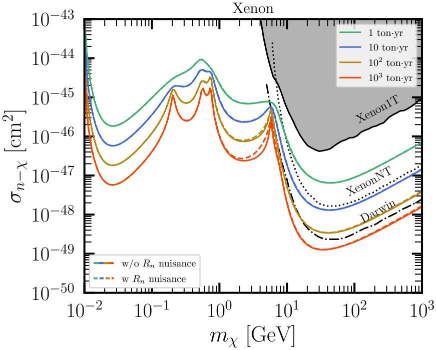

Helm form factor

$$F(q^2) = 3\frac{j_1(qR_0)}{qR_0}\, e^{-\frac{1}{2}(qs)^2}$$

- use $R_p = 4.78$ fm (fixed)
- vary around $R_n = 4.78$ fm (central value)
- assume 10% uncertainty on R_n

- $R_0 = \sqrt{\frac{5}{3}\left(R_X^2 - 3s^2\right)}$
- $s = 0.9$ fm

[Aristizabal, De Romeri, Flores, DKP: 2109.03247 [hep-ph]]

A new scalar boson mediating CEvNS ?

$$\frac{d\sigma_S}{dE_r} = \frac{G_F^2}{2\pi} m_N \mathcal{Q}_S^2 \frac{m_N E_r}{2E_\nu^2} F^2(q^2)$$ [Cerdeno et al. JHEP 05 (2016)]

scalar charge: $$\mathcal{Q}_S = \frac{C_S^N F_S}{G_F(2m_N E_r + m_S^2)}$$

[Aristizabal et al. JHEP 12 (2019)]

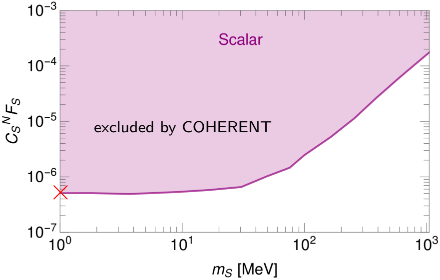

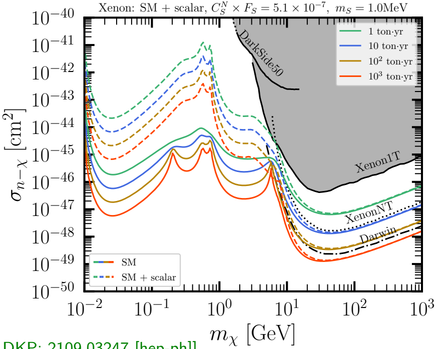

[Aristizabal, De Romeri, Flores, DKP: 2109.03247 [hep-ph]]

A new vector boson mediating CEvNS ?

$$\frac{d\sigma}{dE_r} = \frac{m_N G_F}{2\pi} \mathcal{Q}_V^2 \left(2 - \frac{m_N E_r}{E_\nu^2}\right) F^2(q)$$

[Cerdeno et al. JHEP 05 (2016)]

vector charge: $$\mathcal{Q}_V = \mathcal{Q}_W + \frac{C_V^N F_V}{\sqrt{2} G_F (2 m_N E_r + m_V^2)}$$

[Aristizabal et al. JHEP 12 (2019)]

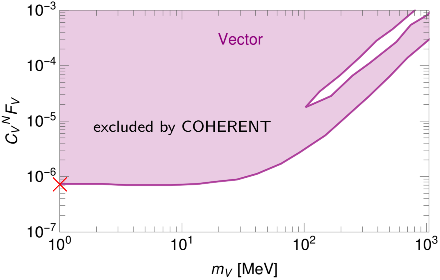

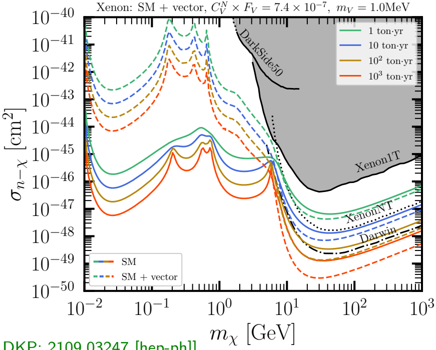

[Aristizabal, De Romeri, Flores, DKP: 2109.03247 [hep-ph]]

Electromagnetic neutrino properties

$$\frac{d\sigma_\gamma}{dE_r} = \pi\alpha_{\text{em}}^2 \, Z^2 \frac{\mu_{\text{eff}}^2}{m_e^2} \left(\frac{1}{E_r} - \frac{1}{E_\nu}\right) F^2(q^2)$$

[Vogel, Engel et al. PRD 39 (1989)]

magnetic moment: μ_ν

[XENON collab. PRD 102 (2020)]

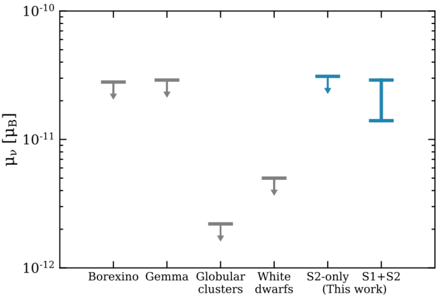

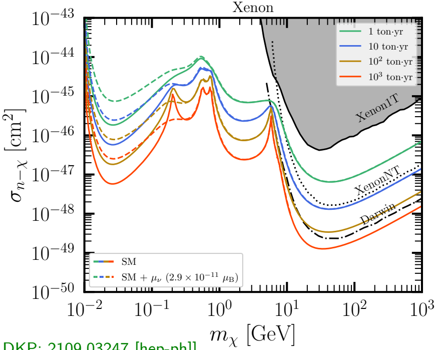

[Aristizabal, De Romeri, Flores, DKP: 2109.03247 [hep-ph]]

Neutrino floor: data-driven analysis

Utilize the measured CEνNS cross section with its uncertainty

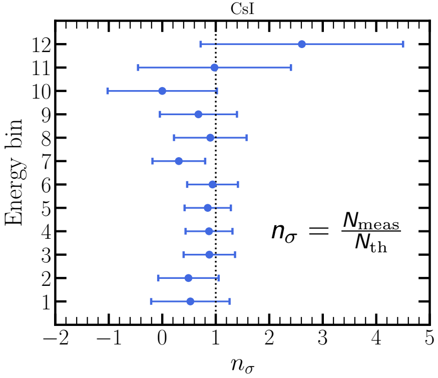

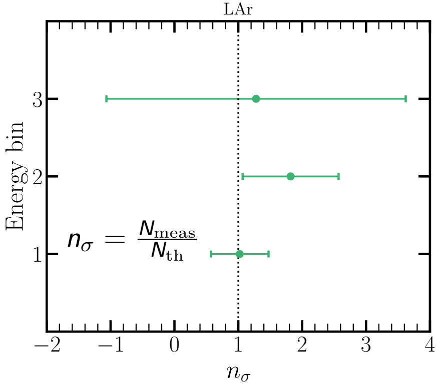

- **what?** extract the CEνNS cross section central values & standard deviations
- **how?** weigh the theoretical SM value of the CEνNS differential cross section with a multiplicative factor *i.e.* $\sigma^i_{\rm meas} = n^i_\sigma \sigma^i_{\rm th}$ and use a spectral χ^2 fit
- **why?** all possible uncertainties that the cross section can involve–independently of assumption–are encoded.

[Aristizabal, De Romeri, Flores, DKP: 2109.03247 [hep-ph]]

Neutrino floor: data-driven analysis

Utilize the measured CEνNS cross section with its uncertainty

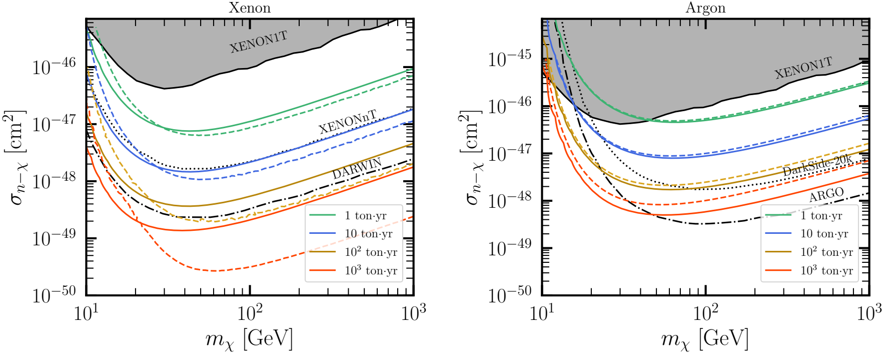

- **analysis of CsI data:** WIMP discovery limits improve compared to the SM expectation (solid curves).
  The measured CEνNS cross section (central values) is smaller than the SM expectation, thus resulting in a background depletion.
- **analysis of LAr data:** Results behave differently.

[Aristizabal, De Romeri, Flores, DKP: 2109.03247 [hep-ph]]

Conclusions: physics potential using CEνNS

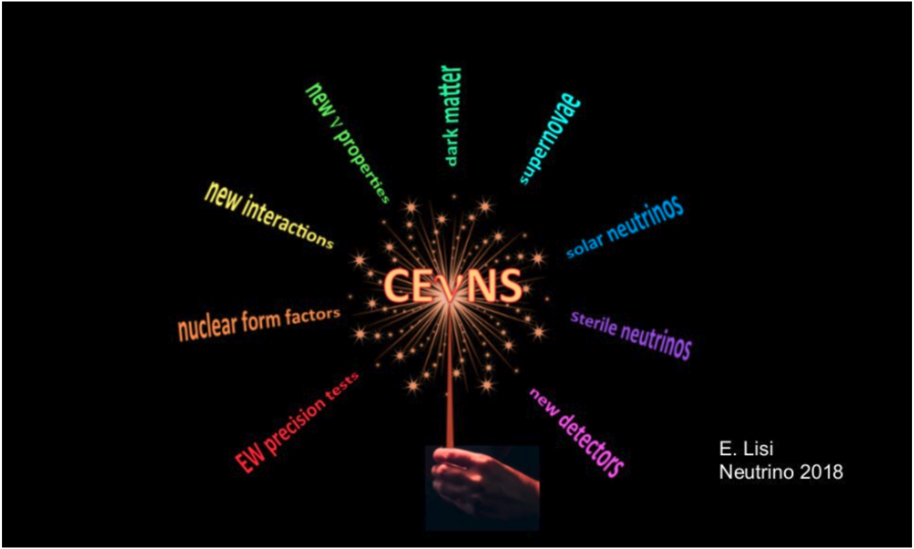

Thank you for your attention !

Extras

Incoherent neutrino-nucleus scattering

Naumov Bednyakov formalism

$$\frac{d\sigma_{\text{inc}}}{dT_A} = \frac{4G_F^2 m_A}{\pi} \sum_{f=n,p} g_{\text{inc}}^f \left(1 - |F_f|^2\right)$$
$$\times \left[A_+^f \left(\left(g_{L,f} - g_{R,f}\, ab^2\right)^2 + g_{R,f}^2\, ab^2 (1-a) \right) + A_-^f g_{R,f}^2 (1-a) \left(1 - a + ab^2\right) \right]. \quad (1)$$

$$a = \frac{q^2}{q^2_{\text{min}}} \simeq \frac{T_A}{T_A^{\text{max}}}, \quad b^2 = \frac{m_f^2}{s}. \quad (2)$$

Here, $A_\pm^p \equiv Z_\pm$ ($A_\pm^n \equiv N_\pm$) represents the number of protons (neutrons) with spin $\pm 1/2$ and $s = (p+k)^2$ is the total energy squared in the center-of-mass frame (p denotes an effective 4-momentum of the nucleon).

[Bednyakov, Naumov, PRD 98 (2018) 053004]

For a more detailed study see: [Hoferichter, Menéndez, Schwenk PRD 102, 074018]

TMMs in flavor & mass basis @ SNS facilities (prompt)

Prompt beam: $\underline{\nu_\mu \text{ (with } \mathfrak{a}_-^2 = 1)}$

- flavor basis

$$\left(\mu^F_{\nu_\mu,\,\mathrm{prompt}}\right)^2 = |\Lambda_e|^2 + |\Lambda_\tau|^2$$

- mass basis

$$\begin{aligned}
\left(\mu^M_{\nu_\mu,\,\mathrm{prompt}}\right)^2 = {} & |\Lambda_1|^2 \left[-2c_{12}c_{23}s_{12}s_{13}s_{23}\cos\delta_{\mathrm{CP}} + s_{23}^2\left(c_{13}^2 + s_{12}^2 s_{13}^2\right) + c_{12}^2 c_{23}^2\right] \\
& + |\Lambda_2|^2 \left[2c_{12}c_{23}s_{13}s_{23}s_{12}\cos\delta_{\mathrm{CP}} + c_{23}^2 s_{12}^2 + s_{23}^2\left(c_{12}^2 s_{13}^2 + c_{13}^2\right)\right] \\
& + |\Lambda_3|^2 \left[c_{23}^2 + s_{13}^2 s_{23}^2\right] \\
& + 2\,|\Lambda_1\Lambda_2| \left[c_{23}c_{12}^2 s_{13}s_{23}\cos\left(\delta_{\mathrm{CP}} + \xi_3\right) - c_{23}s_{12}^2 s_{13}s_{23}\cos\left(\delta_{\mathrm{CP}} - \xi_3\right)\right. \\
& \qquad \left. + c_{12}s_{12}\left(c_{23}^2 - s_{13}^2 s_{23}^2\right)\cos\xi_3\right] \\
& + 2\,|\Lambda_1\Lambda_3| \left[c_{13}s_{23}\left(c_{12}s_{13}s_{23}\cos\left(\delta_{\mathrm{CP}} - \xi_2\right) + c_{23}s_{12}\cos\xi_2\right)\right] \\
& + 2\,|\Lambda_2\Lambda_3| \left[c_{13}s_{23}\left(s_{12}s_{13}s_{23}\cos\left(\delta_{\mathrm{CP}} - \xi_1\right) - c_{12}c_{23}\cos\xi_1\right)\right] .
\end{aligned}$$

[Miranda, DKP, Tórtola, Valle, JHEP 1907 (2019) 103]

TMMs in flavor & mass basis @ SNS facilities (delayed ν_e)

Delayed beam: (i) ν_e (with $\mathfrak{a}_-^1 = 1$) and (ii) $\bar{\nu}_\mu$ (with $\mathfrak{a}_+^2 = 1$)

ν_e component

- flavor basis

$$\left(\mu^F_{\nu_e,\,\text{delayed}}\right)^2 = |\Lambda_\mu|^2 + |\Lambda_\tau|^2$$

- mass basis

$$\begin{aligned}\left(\mu^M_{\nu_e,\,\text{delayed}}\right)^2 = &\ |\Lambda_1|^2 \left[c_{13}^2 s_{12}^2 + s_{13}^2\right] + |\Lambda_2|^2 \left[c_{12}^2 c_{13}^2 + s_{13}^2\right] + |\Lambda_3|^2\, c_{13}^2 \\ &- |\Lambda_1 \Lambda_2| \left[c_{13}^2 \sin(2\theta_{12}) \cos\xi_3\right] - |\Lambda_1 \Lambda_3| \left[c_{12} \sin(2\theta_{13}) \cos(\delta_{\text{CP}} - \xi_2)\right] \\ &- |\Lambda_2 \Lambda_3| \left[s_{12} \sin(2\theta_{13}) \cos(\delta_{\text{CP}} - \xi_1)\right] ,\end{aligned}$$

[Miranda, DKP, Tórtola, Valle, JHEP 1907 (2019) 103]

TMMs in flavor & mass basis @ SNS facilities (delayed $\bar{\nu}_\mu$)

Delayed beam: (i) ν_e (with $\mathfrak{a}_-^1 = 1$) and (ii) $\bar{\nu}_\mu$ (with $\mathfrak{a}_+^2 = 1$)

$\bar{\nu}_\mu$ component

- flavor basis

$$\left(\mu^F_{\bar{\nu}_\mu,\,\text{delayed}}\right)^2 = |\Lambda_e|^2 + |\Lambda_\tau|^2$$

- mass basis

$$\begin{aligned}\left(\mu^M_{\bar{\nu}_\mu,\,\text{delayed}}\right)^2 = {} & |\Lambda_1|^2 \left[-2c_{12}c_{23}s_{12}s_{13}s_{23}\cos\delta_{\text{CP}} + s_{23}^2\left(c_{13}^2 + s_{12}^2 s_{13}^2\right) + c_{12}^2 c_{23}^2\right] \\ & + |\Lambda_2|^2 \left[2c_{12}c_{23}s_{12}s_{13}s_{23}\cos\delta_{\text{CP}} + s_{23}^2\left(c_{13}^2 + c_{12}^2 s_{13}^2\right) + s_{12}^2 c_{23}^2\right] \\ & + |\Lambda_3|^2 \left[\frac{1}{4}\left(2c_{13}^2\cos(2\theta_{23}) - \cos(2\theta_{13}) + 3\right)\right] \\ & + 2\,|\Lambda_1\Lambda_2| \left[c_{23}s_{13}s_{23}\left(c_{12}^2\cos\left(\delta_{\text{CP}} + \xi_3\right) - s_{12}^2\cos\left(\delta_{\text{CP}} - \xi_3\right)\right)\right. \\ & \left. + c_{12}c_{23}^2 s_{12}\cos\xi_3 - c_{12}s_{12}s_{13}^2 s_{23}^2\cos\xi_3\right] \\ & + 2\,|\Lambda_1\Lambda_3| \left[c_{13}s_{23}\left(c_{12}s_{13}s_{23}\cos\left(\delta_{\text{CP}} - \xi_2\right) + c_{23}s_{12}\cos\xi_2\right)\right] \\ & + 2\,|\Lambda_2\Lambda_3| \left[c_{13}s_{23}\left(s_{12}s_{13}s_{23}\cos\left(\delta_{\text{CP}} - \xi_1\right) - c_{12}c_{23}\cos\xi_1\right)\right]\end{aligned}$$

[Miranda, DKP, Tórtola, Valle, JHEP 1907 (2019) 103]

Effective NMM relevant to solar neutrino detection

NMM in the mass basis is known to be

$$\left(\mu_{\nu,\text{eff}}^{M}\right)^{2}(L, E_\nu) = \sum_j \left| \sum_i U_{\alpha i}^{*} e^{-i\,\Delta m_{ij}^2 L/2E_\nu} \tilde{\lambda}_{ij} \right|^2$$

- neutrino mixing and oscillations between the source and detection considered
- Λ_i: entries of the transition magnetic moment matrix with $\lambda_{\alpha\beta} = \varepsilon_{\alpha\beta\gamma}\Lambda_\gamma$

For solar neutrinos (mass basis) [Cañas et al.: PLB 753 (2016)]

$$(\mu_{\nu,\,\text{sol}}^{M})^2 = |\boldsymbol{\Lambda}|^2 - c_{13}^2|\Lambda_2|^2 + (c_{13}^2 - 1)|\Lambda_3|^2 + c_{13}^2 P_{e1}^{2\nu}(|\Lambda_2|^2 - |\Lambda_1|^2)$$

- solar electron neutrinos undergo flavor oscillations arriving to the detector as an incoherent admixture of mass eigenstates (no phase dependence)
- the oscillation probabilities from ν_e to mass eigenstates ν_i are approximated

$$P_{e3}^{3\nu} = \sin^2\theta_{13}, \quad P_{e1}^{3\nu} = \cos^2\theta_{13} P_{e1}^{2\nu}, \quad P_{e2}^{3\nu} = \cos^2\theta_{13} P_{e2}^{2\nu},$$

with the unitarity condition, $P_{e1}^{2\nu} + P_{e2}^{2\nu} = 1$

WIMP-nucleus rates

- differential WIMP-nucleus event rate

$$\frac{dR(u,\upsilon)}{dq^2} = N_t\phi\frac{d\sigma}{dq^2}f(\upsilon)\,d^3\upsilon, \quad \phi = \rho_0\upsilon/m_\chi$$

with the dimensional parameter $u = q^2b^2/2$

ρ_0 is the local WIMP density

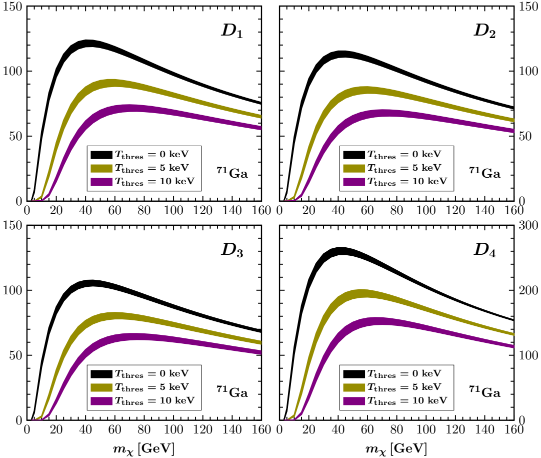

- $f(\upsilon)$: distribution of WIMP velocity (Maxwell-Boltzmann)

for consistency with the LSP

- WIMP-nucleus rate

$$\langle R\rangle = (f_A^0)^2D_1 + 2f_A^0f_A^1D_2 + (f_A^1)^2D_3 + A^2\left(f_S^0 - f_S^1\frac{A-2Z}{A}\right)^2|F(u)|^2D_4\,.$$

with

$$D_i = \int_{-1}^{1}d\xi\int_{\psi_{\rm min}}^{\psi_{\rm max}}d\psi\int_{u_{\rm min}}^{u_{\rm max}}G(\psi,\xi)X_i\,du\,,$$

and

$$X_1 = [\Omega_0(0)]^2\,F_{00}(u)\,,$$
$$X_2 = \Omega_0(0)\Omega_1(0)F_{01}(u)\,,$$
$$X_3 = [\Omega_1(0)]^2\,F_{11}(u)\,,$$
$$X_4 = |F(u)|^2\,.$$

DKP et al., Adv.High Energy Phys. 2018 (2018) 6031362